High-Spin Molecules: A Novel Cyano-Bridged $Mn^{II}_9Mo^{V}_6$ Molecular Cluster with a $S = 51/2$ Ground State and Ferromagnetic Intercluster Ordering at Low Temperatures**

Joulia Larionova, Mathias Gross, Melanie Pilkington, Hanspeter Andres, Helen Stoeckli-Evans, Hans U. Güdel, and Silvio Decurtins*

Dedicated to Professor Andreas Ludi on the occasion of his retirement

The synthesis and investigation of the magnetic properties of novel molecular clusters containing paramagnetic transition metal ions is currently attracting a great deal of interest. This is driven by the ability of selected cluster compounds to function as nanoscale magnets at cryogenic temperatures.[1–18] These molecular compounds are characterized by a ground state with an unusually large number of unpaired electrons. The existence of a fairly large ground state spin (S) value, together with a large magnetic anisotropy is necessary for molecules to exhibit this new magnetic phenomenon of single-molecule magnetism, and accordingly, such high-spin molecules have been termed "single-molecule magnets" (SMM).[12]

The importance of a high S value in molecular compounds has stimulated the search for new SMM, but until now molecules with $S > 10$ are very rare.[1, 9] The highest value reported to date is $S = 33/2$[3] for a cocrystallized Fe_{17} and Fe_{19} species.[9] The most accurately investigated system so far belongs to the series of manganese carboxylates of general formula $[Mn_{12}O_{12}(RCOO)_{16}]$ with a varying number of water molecules.[1–7] These molecules all contain eight Mn^{III} and four Mn^{IV} ions and the acetate derivative is reported to have a ground $S = 10$ state.[2] For this cluster, a slow relaxation of the magnetization was detected at low temperature, similar to the blocking temperature of superparamagnets.[2] Consequently, in the low-temperature regime, this cluster behaves like a single-molecule magnet and shows molecular hysteresis effects. This bistability opens up exciting possibilities for the storage of information at the molecular level.

As research in this field progresses, a question arises, with the realization of cluster compounds with an increasing number of spins, does the S value become so large that we enter the regime where the cluster magnetic characteristics are interwoven with those of the onset of bulk magnetic behavior?

We report herein the structural and magnetic properties of the novel molecular cluster compound **1**, which exhibits the largest spin ground state observed to date. Cluster **1** comprises of fifteen cyano-bridged metal ions, namely nine Mn^{II} ions ($S = 5/2$) and six Mo^{V} ions ($S = 1/2$), giving a total of 51 unpaired electrons. For simplification, the molecular configuration of an idealized pentadecanuclear cluster core with O_h symmetry is sketched in Figure 1. The nine Mn^{II} ions define a body-centered cube, and the six Mo^{V} ions constitute an octahedron.

$$[Mn^{II}\{Mn^{II}(MeOH)_3\}_8(\mu\text{-}CN)_{30}\{Mo^{V}(CN)_3\}_6]\cdot 5\,MeOH\cdot 2\,H_2O \qquad \mathbf{1}$$

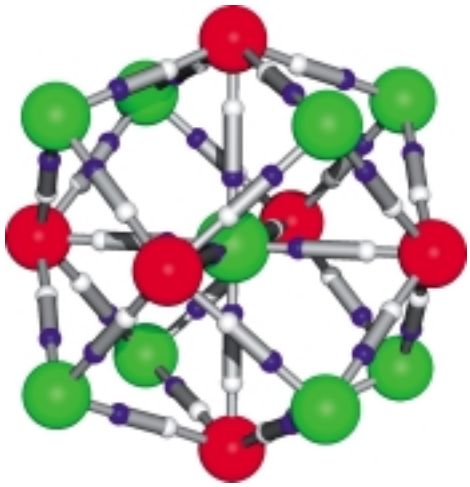

Figure 1. Representation of the $[Mn^{II}_9(\mu\text{-}CN)_{30}Mo^{V}_6]$ cluster core. The figure is drawn for maximal symmetry (O_h) to accentuate the cluster topology. The green spheres represent Mn^{II} ions, the red spheres represent the Mo^{V} ions and the bonds between them represent the μ-cyano ligands.

The central Mn^{II} ion is connected to six Mo^{V} ions by six μ-cyano-ligands. Each of the Mo^{V} ions is linked by four more μ-cyano-ligands to four peripheral Mn^{II} ions. Each of the eight peripheral Mn^{II} ions is connected by μ-cyano-ligands to three Mo^{V} ions, thus the Mn^{II} ions cap the faces of the Mo^{V} octahedron. To summarize, the Mo^{V}-CN-Mn^{II} geometry is such that the atoms are linked to form an aesthetically pleasing topological pattern in which the polyhedron spanned by the peripheral metal ions is closest in geometry to a rhombic dodecahedron. This topology is reminescent of the well documented $[Mo_6X_8]^{4+}$ unit from molybdenum dichloride/dibromide.[19]

The exact molecular geometry of the compound has been determined by single-crystal X-ray analysis at 223 K. (Figure 2). In comparison to the idealized sketch of **1** in Figure 1, the actual cluster has a lower symmetry, C_2, with the central Mn^{II} ion lying on the crystallographic twofold axis. Additional ligands complete the coordination sphere of the peripheral metal ions and complete the charge balance to give a neutral cluster. Three methanol molecules are ligated to the outer Mn^{II} ions, increasing their coordination number to six. Analogously, three additional terminal cyano ligands coor-

[*] Prof. Dr. S. Decurtins, Dr. J. Larionova, M. Gross, Dr. M. Pilkington, H. Andres, Prof. Dr. H. U. Güdel
Departement für Chemie und Biochemie
Universität Bern
Freiestrasse 3, 3012 Bern (Switzerland)
Fax: (+41) 31-631-39-95
E-mail: silvio.decurtins@iac.unibe.ch
Prof. Dr. H. Stoeckli-Evans
Institut de Chimie, Université de Neuchâtel
Avenue Bellevaux 51, 2000 Neuchâtel (Switzerland)

[**] Financial support by the Swiss National Science Foundation through Project No. 21-52699.97 and the TMR Research Network ERBFMRXCT 980181 of the European Union, entitled: "Molecular Magnetism: From Materials towards Devices" is gratefully acknowledged. The authors also thank Thierry Strässle from the Paul Scherrer Institute, Villigen, for assistance with the heat capacity measurement and Professor Fernando Palacio, University of Zaragoza, for stimulating discussions.

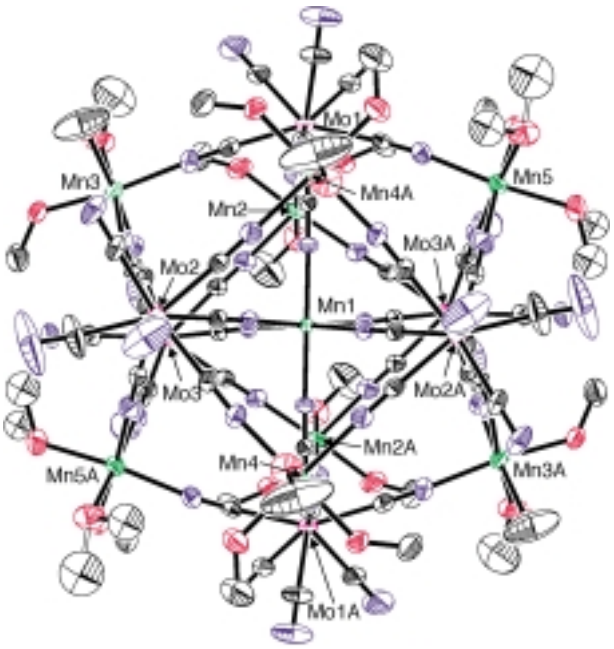

Figure 2. ORTEP representation (ellipsoids at 30% probability) of the molecular structure of **1**; for clarity only the Mn^{II} and Mo^{V} atoms are labeled and the H atoms are omitted. Ranges for selected distances [Å] and angles [°] are given below (the indices c, p, and t represent an atom linked to the center of the cluster, a peripheral atom, and a terminal atom, respectively). The average bond lengths and angles are given in square brackets after the ranges: Mo-C_c 2.13–2.14 [2.14], Mo-C_p 2.14–2.17 [2.15], Mo-C_t 2.13–2.17 [2.14], Mn1-N_c 2.18–2.19 [2.19], Mn-N_p 2.19–2.23 [2.21], Mn-O 2.16–2.20 [2.19], C_c-N_c 1.14–1.15 [1.15], C_p-N_p 1.13–1.15 [1.15], C_t-N_t 1.12–1.16 [1.14], Mn1-Mo 5.47–5.48 [5.47], Mn-Mo 5.47–5.52 [5.49]; C_c-Mo-C_p 70.9–74.6 [72.9], C_p-Mo-C_p 76.0–99.5 [85.0], N_c-Mn1-N_c 85.8–95.1 [90.1], N_c-Mn1-N_c 173.9–175.6 [174.5], N_p-Mn-N_p 90.5–99.0 [93.5].

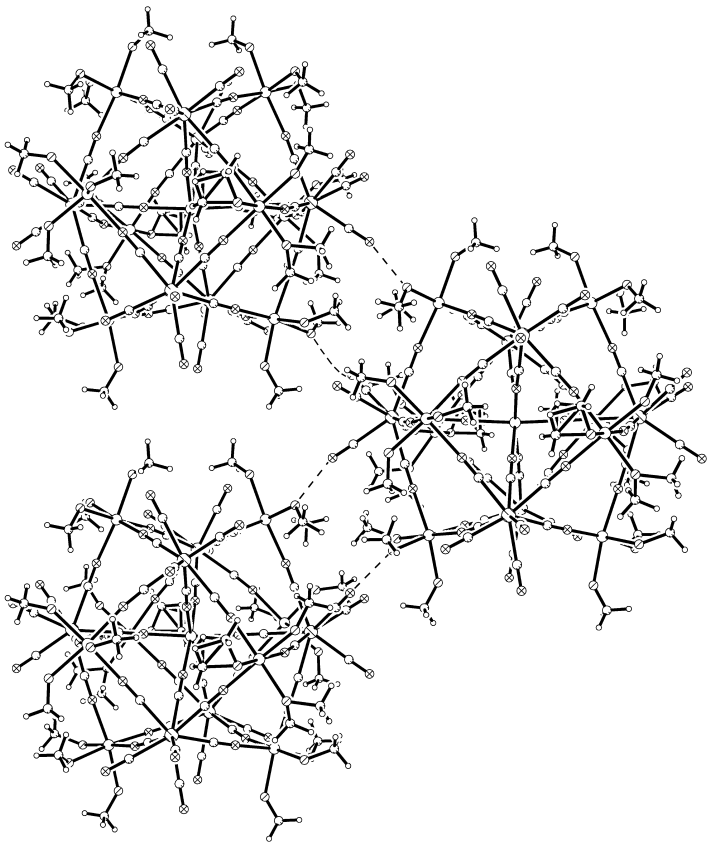

Figure 3. A plot of three nearest neighbor cluster molecules showing the close edge contacts between the Mn^{II} and the Mo^{V} ions. The dotted lines represent the H-bonding interactions O–H···N.

dinate to each Mo^{V} ion establishing an eightfold coordination and giving the overall $[Mo^{V}(CN)_8]^{3-}$ stoichiometry. Two types of geometry for the Mo-C-N-Mn bridges are found in **1**. Those involving the central Mn^{II} ion are fairly linear (Mn-N-C 175.8–179.2° and Mo-C-N 178.1°–179.0°), whereas the peripheral Mo-C-N-Mn bridges are essentially linear at the cyanide carbon (Mo-C-N 175.9–179.8°), but bent at the cyanide nitrogen (Mn-N-C 169.6–178.8°).

The spin-bearing centers in the cluster (with the exception of the central Mn^{II} ion) are all located at the periphery of the molecule and are essentially free from shielding by bulky organic ligands. This is in contrast to many of the high-nuclearity cluster compounds previously reported,[1–18] in which the magnetic intercluster interactions are often efficiently suppressed by a layer of organic ligands.

Compound **1** crystallizes in a monoclinic space group (*C*2/*c*). An extended intermolecular H-bonded network connects each cluster to eight nearest neighbors; Figure 3 shows the H-bond interactions between three of them. Each peripheral Mn^{II} ion of a cluster has one MeOH ligand which is involved in an intermolecular H-bond to the nitrogen atom of a cyano-ligand of a neighboring cluster (terminally attached to a Mo^{V}). For two of the Mo^{V} ions, there are two terminal cyano ligands involved in intermolecular H-bonding interactions with neighboring methanol ligands ligated to Mn^{II} ions of different clusters. The remaining four Mo^{V} ions have one terminal cyano ligand which takes part in an intermolecular H-bonding interaction with a neighboring methanol ligand. Thus, each cluster is involved in sixteen H-bonding interactions with its nearest neighbors. All of these O–H···N contacts are in the range 2.70–2.76 Å and are well within the sum of the van der Waals radii (2.9 Å), indicative of 'medium strength' hydrogen bonds. This extended intercluster H-bonded network, in which the MeOH donors and CN acceptors are connected in a regular donor-acceptor sequence to give a continuous three dimensional (3D) array, results in close nearest neighbor contacts between metal ions at the edges of the clusters (Mo–Mn 6.97–7.58, Mn–Mn 7.20–7.58 Å). All remaining cyano and methanol ligands not involved in intercluster H-bonding interactions form hydrogen bonds with neighboring solvent molecules. The solvent molecules (MeOH and H_2O) occupy channels between the clusters, filling up the remaining unoccupied space in the crystal lattice.

Cyano-bridged metal assemblies are not new to the field of molecular magnetism, and several examples using cyano-bridged coordination to build up extended networks displaying interesting magnetic and photomagnetic properties have been reported.[20–22]

Having synthesized and structurally characterized a molecular compound possessing 51 unpaired electrons, we focused our attention on the magnetic behavior of **1**. Variable temperature dc–magnetic susceptibility studies were carried out to determine the spin value for the ground state of **1**. Data

  0570-0833/00/3909-1606 $ 17.50+.50/0

were collected in the temperature range 1.8–300 K for polycrystalline samples, and in preliminary studies on oriented single crystals. In addition, heat capacity measurements were carried out on single crystals in the temperature range 1.8–100 K. First, we dicuss the high-temperature regime, namely $50 < T < 300$ K. Figure 4 shows the corresponding plot of $\chi_m T$ versus T, which demonstrates a gradual increase of $\chi_m T$ with the lowering of temperature. This behavior indicates the presence of ferromagnetic intracluster exchange interactions. Even at 300 K, the experimental value of $\chi_m T = 46$ emu K mol^{-1} is slightly higher than the calculated spin-only value of $\chi_m T = 40.9$ emu K mol^{-1} for a cluster comprising nine noninteracting Mn^{II} ($g = 2.0$, $S = 5/2$) and six noninteracting Mo^{V} ($g = 1.98$, $S = 1/2$)[23] centers, demonstrating the effect of the ferromagnetic intracluster exchange. In conclusion, the magnetic behavior of this compound at $T > 50$ K is dominated by intracluster exchange interactions.

To obtain a rough quantitative estimate of the intracluster exchange interaction parameter J, calculations based on the Hamiltonian $\mathscr{H} = -2J\boldsymbol{S}_{Mn}\boldsymbol{S}_{Mo}$ were performed. In these calculations we assume only one type of Mn-NC-Mo nearest neighbor interaction and consequently, the temperature dependence of $\chi_m T$ is only a function of one single energy parameter, namely J. Despite this simplicity, the calculation of $\chi_m T$ versus T for the whole pentadecanuclear cluster is still beyond our reach, since the total number of electronic cluster states is simply too large, being of the order of 10^7. As a consequence of this, we selected three cluster fragments of increasing size, as shown in Figure 4 and calculated $\chi_m T$ for various J values using a reported algorithm.[24] From a

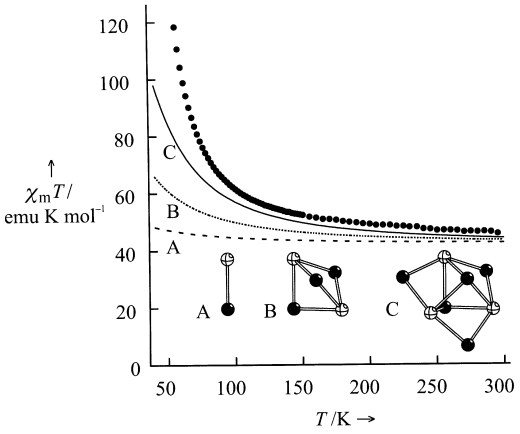

Figure 4. Temperature dependence of $\chi_m T$ above 50 K for the polycrystalline cluster compound **1**. The lines A–C represent calculated results (see text) for the corresponding cluster fractions (Mn^{II}: dark spheres; Mo^{V}: light spheres) using $J = 7$ cm^{-1}.

comparison with the experimental data and considering an extrapolation to the pentadecanuclear cluster unit, a ferromagnetic exchange interaction parameter J of 7 cm^{-1} is deduced as an upper limit. For example, for $J = 4$ cm^{-1}, the total energy spread of the exchange-split ground state of the $Mn^{II}_9Mo^{V}_6$ cluster is in the order of 500 cm^{-1}. Thus, even at room temperature, there is no complete thermalization within the ground-state multiplet and this is in good agreement with the observed $\chi_m T$ value of 46 emu K mol^{-1}.

Figure 5 shows the plot of $\chi_m T$ versus T for different values of the applied field for the low-temperature regime, $T < 50$ K. Most significantly, the gradual increase of $\chi_m T$ with the lowering of temperature shows a clear break around 44 K, where $\chi_m T$ starts to rise steeply to over 4×10^4 emu K mol^{-1} for an applied field of 1.5 G. This abrupt increase of $\chi_m T$ indicates the onset of cooperative ferromagnetic intercluster

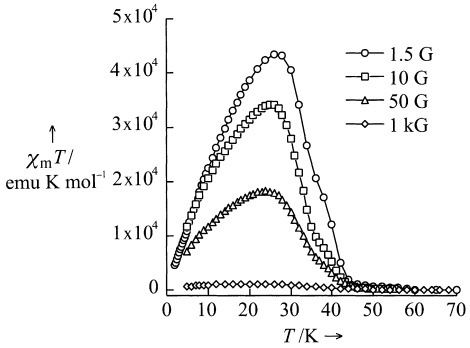

Figure 5. Temperature dependence of $\chi_m T$ below 70 K for the polycrystalline cluster compound **1** at different field values.

interactions. For comparison, the calculated $\chi_m T$ value for magnetically isolated exchange coupled clusters with $S = 51/2$ ground state spin would be only 338 emu K mol^{-1}. The magnetic susceptibility below 44 K is strongly field dependent, indicating the possibility of competing effects between the external field and the intercluster interactions. In addition, preliminary measurements on oriented single crystals show the magnetic susceptibility at $T < 44$ K to be clearly dependent on the crystal orientation relative to the applied field. All these results indicate that on lowering the temperature the magnetic cluster signature is lost and below 44 K a bulk behavior starts to emerge. This relatively high onset of intercluster correlations can be due to both exchange and magnetic dipole–dipole interactions. The former are facilitated by the sixteen hydrogen bonds per cluster between the terminal cyano and MeOH ligands of neighboring cluster molecules. For the latter, the isotropic interaction energy between two magnetic dipoles of $S = 51/2$ separated by 17.5 Å, that is the distance between the centers of nearest neighbor clusters, is of the order of 0.2 cm^{-1}.[25] The estimate of 0.2 cm^{-1} is valid at the very lowest temperatures with only the $S = 51/2$ cluster level populated. Around 40 K it is definitely lower because of the population of cluster levels with lower S values. From a calculation on the cluster fragments in Figure 4, a mean spin value of about $S = 12$ can be extrapolated for the whole cluster. This S value results in a magnetic dipolar interaction energy of the order of 0.05 cm^{-1}. Using these values and the molecular-field approximation, we estimate a T_C of about 30 K. This is in reasonably good agreement with the observed onset of cooperative intercluster correlations around 40 K. We conclude that magnetic dipolar interactions account for the major part of intercluster correlations in this temperature range.

A plot of χ_m^{-1} versus T shows linear behavior between 300 and 120 K (Curie constant $C = 41.8$ emu K mol^{-1}) which extrapolates to a positive Curie–Weiss constant Θ of 30.4 K.

  0570-0833/00/3909-1607 $ 17.50+.50/0

This positive value is also related to the presence of ferromagnetic exchange interactions.

To confirm the characteristic behavior of the ferromagnetically correlated phase, the temperature dependences of the magnetization M under a weak magnetic field (1 G) and the remanent magnetization were measured. The field-cooled magnetization (FCM), zero-field-cooled magnetization (ZFCM) and remanent magnetization (RM) curves are shown in Figure 6. The FCM obtained by cooling the sample under

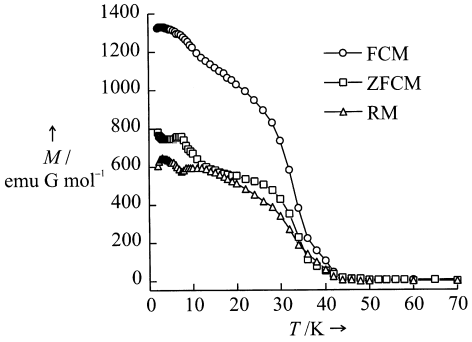

Figure 6. Temperature dependence of the magnetization M for the polycrystalline cluster compound **1** with FCM, (H = 1 G), ZFCM, and RM measuring protocols.

1 G shows a rapid increase when the temperature is lowered below 44 K and has inflection points around 35 K and 8 K. When the field was switched off at 1.8 K, a remanent magnetization was observed which vanished as the temperature was increased to 44 K. If the inflection point at 35 K is attributed to a distinct 3D ferromagnetic phase transition, the remanent magnetization should vanish at that temperature. Analogously, the ZFCM (cooling in zero field and warming under 1 G) would be expected to merge with the FCM curve at 35 K. This is not strictly, but approximately observed in Figure 6.

In addition (Figure 7) a sharp λ-peak appears in the heat capacity measurement at 2.9 K . Considering the very high spin value of $S = 51/2$, only a relatively low experimental

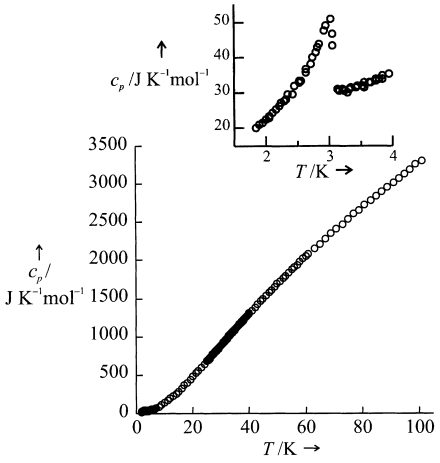

Figure 7. Temperature dependence of the molar heat capacity c_p for the crystalline cluster compound **1**.

magnetic heat capacity contribution C_m of 1.3 R is observed, indicating that the substantial part of the magnetic intercluster correlation occurs between 44 and 2.9 K. This low value can be compared with the experimental C_m of 2.8 R for another molecular ferromagnetic material ($T_C = 6$ K) where, within an extended 2D network, Mn^{II} ions ($S = 5/2$) and Cr^{III} ions ($S = 3/2$) are bridged by μ-oxalato ligands.[26] The nature of the transition at 2.9 K is not yet understood.

Finally, the magnetization data collected at several temperatures between 2 K and 60 K with applied fields up to 50 kG are shown in Figure 8. The curve at 2 K exhibits a very high zero-field susceptibility and reaches a saturation value near

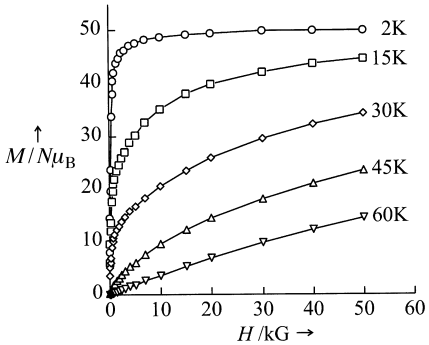

Figure 8. Field dependence of the magnetization M for the polycrystalline cluster compound **1** at different temperatures.

the expected $M_S/N\mu_B$ value of 51 for a $S = 51/2$ ground state, calculated with a value of g(cluster) = 2.0. In addition, a very narrow hysteresis loop was observed at 2 K with a coercive field of 15 G. A clear change in the shape of the magnetization curves taken below and above 44 K is observed; below 44 K, a high zero-field susceptibility value appears, whereas above 44 K this signature of ferromagnetic intercluster interactions is missing.

In summary, we have prepared and magnetically characterized a new compound containing high-spin clusters with a $S = 51/2$ ground state. In contrast to other high-spin clusters, such as Mn_{12} acetate,[2] compound **1** does not exhibit the typical phenomena of molecular hysteresis and slow quantum tunneling at low temperatures. In **1**, a competitive interplay of intra- and intercluster interactions leads to a very interesting magnetic regime in the temperature range below 44 K. Magnetic dipole–dipole as well as exchange interactions may contribute to the intercluster coupling in **1**. It is clear that dipole–dipole intercluster interactions will become increasingly important with increasing ground state S values of high-spin clusters; it will therefore be increasingly difficult to observe typical nano-magnetic properties of spin clusters, unless specific measures are taken to isolate and insulate them.

In compound **1**, the magnetic properties above 44 K are characterized by ferromagnetic intracluster coupling. Extraction of J values requires approximation techniques, by which we obtain 7 cm^{-1} as an upper limit. A modeling of the magnetic data below 44 K, where magnetic ordering seems to arrive, is not possible at present because this new and interesting situation has not been dealt with theoretically so far.

  0570-0833/00/3909-1608 $ 17.50+.50/0

Experimental Section

Compound **1** was obtained from the reaction of a 3:2 molar ratio of $[Mn^{II}(H_2O)_6](NO_3)_2 \cdot x\,H_2O$ and $(NBu_4)_3[Mo^{V}(CN)_8]$ in a (1:1) methanol/propanol mixture at room temperature.[27] After a few days, dark red-brown crystals with an elongated polyhedral shape formed. The compound is fairly air and light sensitive, so all physical measurements were performed in the dark with polycrystalline material or single-crystals embedded in a grease envelope. The composition of the crystalline compound was established by single-crystal X-ray diffraction at 223 K.

Magnetic susceptibility data were collected with a Quantum Design SQUID magnetometer (XL5S) in the temperature range of 300 – 1.8 K. The output data were corrected for the diamagnetism of the samples and the sample holder as well as for a temperature independent paramagnetism (TIP) contribution (estimated to be 3×10^{-3} emu mol^{-1} per formula unit). Heat capacity data were taken on single crystals with a Quantum Design Physical Property Measurement System (PPMS) (6000/6500) in the temperature range 100 – 1.8 K.

X-ray structure analysis for **1**: $M_r = 3284.31$, crystal dimensions $0.7 \times 0.6 \times 0.4$ mm^3, monoclinic, space group $C2/c$, $a = 29.3847(18)$, $b = 19.3861(11)$, $c = 32.8841(11)$ Å, $\beta = 114.188(6)^\circ$, $V = 17088.0(15)$ Å^3, $Z = 4$, $\rho_{calcd} = 1.277$ g cm^{-3}, $\mu(Mo_{K\alpha}) = 1.126$ mm^{-1}, $2\theta_{max} = 44.66^\circ$, $T = 223(2)$ K. Intensity data were collected on a Stoe Image Plate diffraction system equipped with a Φ circle, using $Mo_{K\alpha}$ graphite-monochromated radiation ($\lambda = 0.71073$ Å) with an image plate distance of 90 mm, ϕ range 0 – 200°, increment 1.0°, θ range 1.66 – 22.33°, $D_{max} - D_{min}$ 16.00 – 0.93 Å. A total of 36821 reflections were measured, of which 10834 independent ($R_{int} = 0.0836$), and 9146 independent for $I > 2\sigma(I)$. The structure was solved by direct methods using the program SHELXS-97.[28] The refinement and all further calculations were carried out using SHELXL-97.[29] An empirical (DIFABS) correction was applied ($R_{int} = 0.0488$). Hydrogen atoms were included in calculated positions and treated as riding atoms using SHELXL-97 default parameters. The majority of the non-H atoms were refined anisotropically, using weighted full-matrix least-squares on F^2. Certain coordinated methanol ligands are disordered with the C atoms occupying two alternative positions and these atoms were refined isotropically. In the final rounds of refinement the solvent molecules of crystallization (CH_3OH and H_2O) were held fixed; 716 refined parameters, $R1 = 0.0458$, $wR2 = 0.1345$ for $I > 2\sigma(I)$ data (without DIFABS these values were 0.0476 and 0.1425, respectively). In general the light atoms in the structure undergo considerable thermal disorder. This is reflected in a certain deviation from the expected values for the C–N (mean value 1.14(2) Å) and C–O (mean value 1.39(11) Å) bond lengths of the groups on the peripheral of the cluster. The cluster molecule possesses crystallographic C_2 symmetry. In the crystal there are two molecules of water and five molecules of methanol per molecule of cluster. The water H-atoms and the methanol hydroxyl H-atoms could not be located. Crystallographic data (excluding structure factors) for the structure reported in this paper has been deposited with the Cambridge Crystallographic Data Centre as supplementary publication no. CCDC-136762. Copies of the data can be obtained free of charge on application to CCDC, 12 Union Road, Cambridge CB2 1EZ, UK (fax: (+44) 1223-336-033; e-mail: deposit@ccdc.cam.ac.uk).

Received: November 19, 1999 [Z14297]

[1] P. D. W. Boyd, Q. Li, J. B. Vincent, K. Folting, H. R. Chang, W. E. Streib, J. C. Huffman, G. Christou, D. Hendrickson, *J. Am. Chem. Soc.* **1988**, *110*, 8537 – 8539.

[2] A. Caneschi, D. Gatteschi, R. Sessoli, A. L. Barra, L. C. Brunel, M. Guillot, *J. Am. Chem. Soc.* **1991**, *113*, 5873 – 5874.

[3] R. Sessoli, D. Gatteschi, A. Caneschi, M. A. Novak, *Nature* **1993**, *365*, 141 – 143.

[4] R. Sessoli, H. L. Tsai, A. R. Schake, S. Wang, J. B. Vincent, K. Folting, D. Gatteschi, G. Christou, D. Hendrickson, *J. Am. Chem. Soc.* **1993**, *115*, 1804 – 1816.

[5] H. J. Eppley, H. L. Tsai, N. De Vries, K. Folting, G. Christou, D. Hendrickson, *J. Am. Chem. Soc.* **1995**, *117*, 301 – 317.

[6] L. Thomas, F. Lionti, R. Ballou, D. Gatteschi, R. Sessoli, B. Barbara, *Nature* **1996**, *383*, 145 – 147.

[7] A. L. Barra, D. Gatteschi, R. Sessoli, *Phys. Rev. B* **1997**, *56,* 8192 – 8198.

[8] D. Gatteschi, A. Caneschi, L. Pardi, R. Sessoli, *Science* **1994**, *265,* 1054 – 1058.

[9] A. K. Powell, S. L. Heath, D. Gatteschi, L. Pardi, R. Sessoli, G. Spina, F. Del Giallo, F. Pieralli, *J. Am. Chem. Soc.* **1995**, *117*, 2491 – 2502.

[10] M. A. Novak, R. Sessoli, A. Caneschi, D. Gatteschi, *J. Magn. Magn. Mater.* **1995**, *146*, 211 – 213.

[11] A. L. Barra, A. Caneschi, D. Gatteschi, R. Sessoli, *J. Am. Chem. Soc.* **1995**, *117*, 8855 – 8856.

[12] S. M. J. Aubin, M. W. Wemple, D. M. Adams, H. L. Tsai, G. Christou, D. Hendrickson, *J. Am. Chem. Soc.* **1996**, *118*, 7746 – 7754.

[13] S. M. J. Aubin, N. R. Dilley, M. W. Wemple, M. B. Maple, G. Christou, D. Hendrickson, *J. Am. Chem. Soc.* **1998**, *120*, 839 – 840.

[14] S. M. J. Aubin, N. R. Dilley, L. Pardi, J. Krzystek, M. W. Wemple, L. C. Brunel, M. B. Maple, G. Christou, D. Hendrickson, *J. Am. Chem. Soc.* **1998**, *120*, 4991 – 5004.

[15] S. L. Castro, Z. Sun, C. M. Grant, J. C. Bollinger, D. Hendrickson, G. Christou, *J. Am. Chem. Soc.* **1998**, *120*, 2365 – 2375.

[16] A. L. Barra, A. Caneschi, A. Cornia, F. Fabrizi de Biani, D. Gatteschi, C. Sanggregorio, R. Sessoli, L. Sorace, *J. Am. Chem. Soc.* **1999**, *121*, 5302 – 5310.

[17] Y. Pontillon, A. Caneschi, D. Gatteschi, R. Sessoli, E. Ressouche, J. Schweizer, E. Lelievre-Berna, *J. Am. Chem. Soc.* **1999**, *121*, 5342 – 5343.

[18] G. Aromi, M. J. Knapp, J. P. Claude, J. C. Huffman, D. Hendrickson, G. Christou, *J. Am. Chem. Soc.* **1999**, *121*, 5489 – 5499.

[19] N. N. Greenwood, A. Earnshaw, *Chemie der Elemente*, VCH, Weinheim, **1990**, p. 1314.

[20] S. Ferlay, T. Mallah, R. Ouahes, P. Veillet, M. Verdaguer, *Nature* **1995**, *378*, 701 – 703.

[21] O. Sato, Y. Einaga, A. Fujishima, K. Hashimoto, *Inorg. Chem.* **1999**, *38*, 4405 – 4412.

[22] O. Kahn, J. Larionova, L. Ouahab, *Chem. Commun.* **1999**, 945 – 952.

[23] S. G. Vulfson, *Molecular Magnetochemistry*, Gordon and Breach Science Publishers, Amsterdam, **1998**.

[24] J. J. Borras-Almenar, J. M. Clemente-Juan, E. Coronado, B. S. Tsukerblat, *Inorg. Chem.* **1999**, *38*, 6081 – 6088.

[25] D. Altbir, P. Vargas, J. d'Albuquerque e Castro, U. Raff, *Phys. Rev. B* **1998**, *57*, 13604 – 13609.

[26] G. Antorrena, F. Palacio, M. Castro, R. Pellaux, S. Decurtins, *J. Magn. Magn. Mater.* **1999**, *196 – 197*, 581 – 583.

[27] N. H. Furman, C. O. Miller in *Inorg. Synthesis, Vol. III* (Ed.: L. F. Audrieth), McGraw-Hill, New York, **1950**, pp. 160 – 163.

[28] G. M. Sheldrick, *Acta Crystallogr. Sect. A* **1990**, *46*, 467 – 473.

[29] G. M. Sheldrick, SHELXL-97, Program for Crystal Structure Refinement, Universität Göttingen (Germany), **1997**.